Nonholonomic Behavior in Free-floating Space Manipulators and its Utilization

Evangelos G. Papadopoulos
McGill Research Centre for Intelligent Machines
3480 University St., Montreal, PQ, Canada H3A 2A7

Abstract

The kinematics and dynamics of free-floating manipulators are examined from a fundamental point of view. The dynamic coupling between an uncontrolled spacecraft and its manipulator can make a system dynamically singular at configurations which cannot be predicted by the system's kinematic properties. Nonholonomic behavior is observed in free-floating systems, and is due to the nonintegrability of the angular momentum. A workspace point can be singular or not, depending on the path taken to reach it. Trouble-free Path Independent Workspaces are defined. Nonholonomy in space manipulators is utilized by planning techniques that permit the control of a spacecraft's attitude by means of joint manipulator motions, the simultaneous control of the joint angles of a manipulator and of the attitude of its spacecraft, using joint motions only, and finally, the effective use of a system's reachable workspace by planning paths that avoid dynamically singular configurations.

I. Introduction

Space robotic devices are envisioned to assist in the construction, repair and maintenance of future space stations and satellites. To increase the mobility of such devices, *free-flying* systems in which one or more manipulators are mounted on a

thruster-equipped spacecraft, have been proposed [1-6]. In such a system, dynamic

coupling between the manipulator and its spacecraft exists, and manipulator motions induce disturbances to the system's spacecraft. Thruster jets can compensate for these disturbances, but their extensive use limits severely a system's useful life span [2-4]. To increase a system's life, operation in a *free-floating* mode has been considered [3-6]. In this mode of operation, spacecraft thrusters are turned off, and the spacecraft is permitted to translate and rotate in response to its manipulator motions. In practice, this mode of operation can be feasible if the total system momentum is zero; if nonzero momentum develops, the system's thrusters must be used to eliminate it.

Free-floating systems exhibit nonholonomic behavior, which is due to the nonintegrability of the angular momentum [8,11]. This property complicates the planning and control of such systems. Joint space planning techniques that take advantage of the nonholonomy in such systems were proposed [2,7,8]. A Self Correcting Planning technique allows the control of a spacecraft's attitude using the manipulator's joint motions [2]. Lyapunov techniques were explored to achieve simultaneous control of a spacecraft's attitude and its manipulator's joint angles, using the manipulator's actuators only. Convergence problems were reported in some cases [7,8]. Various control algorithms were designed for the motion control of free-floating systems, and some of them were experimentally verified [4,5]. However, control algorithm instabilities were observed, [6], which were shown to be due to the existence of dynamic singularities [9,11].

In this paper, the fundamental kinematic and dynamic nature of free-floating manipulators is analyzed, and the nonintegrability of the angular momentum is discussed. Based on this analysis, the controllability of a free-floating system is examined in the joint and Cartesian space. It is shown that a free-floating manipulator is controllable in its joint space, but can be locally uncontrollable in the Cartesian workspace. This is due to the existence of *dynamic singularities*. Unlike to fixed-based systems, dynamically singular configurations cannot be predicted by the kinematic structure of the system, and instead depend upon its mass properties. It is shown that dynamic singularities are *path dependent* and a particular workspace point can induce a dynamic singularity or not, depending upon the path taken to reach it. Path Independent Workspaces are defined as the regions in which no dynamic singularities occur. It is shown that the nonintegrability of the angular momentum introduces nonholonomic behavior in free-floating systems. Joint space path planning techniques that take into advantage the nonholonomic behavior of free-floating systems, like the Self Correcting Planning technique, and Lyapunov-based techniques, are reviewed. Potential problems in using these techniques are identified. Finally, a Cartesian space path-planning technique is presented. This technique avoids dynamically singular configurations, and hence permits the effective use of the full reachable workspace of a free-floating system.

II. Kinematic and Dynamic Modeling of Free-floating Manipulators

A. Kinematic Modelling

This section develops the kinematic and dynamic equations needed to model a rigid free-floating manipulator system, see Figure 1. A key feature of this modeling is expressing the key kinematic and dynamic variables of the system as functions of a set of constant length, body-fixed *barycentric vectors*. The dynamics are written using a Lagrangian approach.

The body 0 in Figure 1 represents the spacecraft; the bodies k (k=1,...,N) represent the N manipulator links. N+1 reference frames are introduced, each one attached to the Center of Mass (*CM*) of each body, with axes parallel to the body's principal axes. Hence, the body inertia matrix expressed in this frame is diagonal. The manipulator joint angles and velocities are represented by the N×1 column vectors $\mathbf{q}$ and $\dot{\mathbf{q}}$. The spacecraft can translate and rotate in response to manipulator movements. The manipulator is assumed to have revolute joints and an open chain kinematic configuration so that, in a system with an N degree-of-freedom (DOF) manipulator, there will be 6+N DOF.

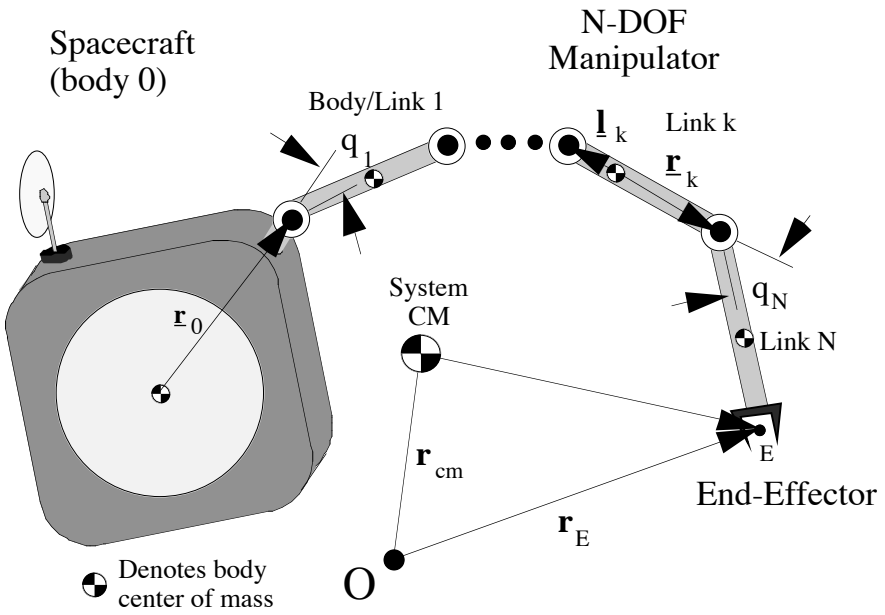

Figure 1. A spatial free-floating manipulator system.

First, the end-effector position, $\mathbf{r}_E$, is written with respect to the inertially fixed origin **O**. It can be shown that $\mathbf{r}_E$ is given by [10,11]:

$$\mathbf{r}_E = \mathbf{r}_{cm} + \sum_{i=0}^{N} \mathbf{v}_{iN} + \mathbf{r}_N = \mathbf{r}_{cm} + \sum_{i=0}^{N} \mathbf{v}_{iN,E} \tag{1}$$

where $\mathbf{r}_{cm}$ is the position vector of the system's *CM* with respect to the origin **O**, vectors $\mathbf{v}_{iN}$ are barycentric vectors fixed on body i, and given in Appendix A by Equation (A1), $\mathbf{r}_N$ is the vector from the *CM* of the last link to the end-effector, and $\mathbf{v}_{iN,E} = \mathbf{v}_{iN} + \delta_{iN}\,\mathbf{r}_N$, where δ_{iN} is the Kronecker's delta, [12,13,11]. Assuming that no external forces act on the system, the system *CM* does not accelerate, and the system linear momentum $\mathbf{p} = M\dot{\mathbf{r}}_{cm}$ is constant. With the further assumption of zero initial linear momentum, $\mathbf{r}_{cm}$ is also a constant, and can be taken to be zero without loss of generality.

The orientation of link i is described by the transformation matrix $\mathbf{T}_i$, given by:

$$\mathbf{T}_i(\boldsymbol{\theta}, q_1,..., q_i) \;=\; \mathbf{T}_0(\boldsymbol{\theta})\;{}^0\mathbf{T}_i(q_1,..., q_i) \tag{2}$$

where $\boldsymbol{\theta}$ represents the orientation of the spacecraft, $\mathbf{T}_0$ is a 3×3 transformation matrix that describes the orientation of the spacecraft frame with respect to the inertial frame, and ${}^0\mathbf{T}_i$ is a 3×3 transformation matrix, function of the joint angles $(q_1,\ldots, q_i)$, that describes the orientation of the i^{th} frame with respect to the spacecraft frame. The orientation of the N^{th} link, is the orientation of the end-effector.

The end-effector inertial linear velocity, $\dot{\mathbf{r}}_E$, is obtained by differentiation of Equation (1). Since the barycentric vectors are body-fixed, $\dot{\mathbf{r}}_E$ is given simply by:

$$\dot{\mathbf{r}}_E \;=\; \dot{\mathbf{r}}_{cm} + \sum_{i=0}^{N} \boldsymbol{\omega}_i^{\times}\mathbf{v}_{iN,E} \;=\; \sum_{i=0}^{N} \boldsymbol{\omega}_i^{\times}\mathbf{v}_{iN,E} \tag{3}$$

where $\boldsymbol{\omega}_i$ is the inertial angular velocity of body i, $\dot{\mathbf{r}}_{cm}$ is the velocity of the system's *CM* taken equal to zero, and the $^{\times}$ converts a vector to the cross-product skew-symmetric matrix, see Equation (A4). The inertial angular velocity $\boldsymbol{\omega}_k$ is written as a function of the spacecraft's angular velocity expressed in the 0^{th} frame, ${}^0\boldsymbol{\omega}_0$, and the manipulator joint rates, $\dot{\mathbf{q}}$:

$$\boldsymbol{\omega}_k \;=\; \mathbf{T}_0\,({}^0\boldsymbol{\omega}_0 + {}^0\mathbf{F}_k\,\dot{\mathbf{q}}) \qquad\qquad k = 1,\ldots,N \tag{4}$$

where ${}^0\mathbf{F}_k$ is a 3×N matrix given by:

$${}^0\mathbf{F}_k \;\equiv\; [\,{}^0\mathbf{T}_1\,{}^1\mathbf{u}_1,\; {}^0\mathbf{T}_2\,{}^2\mathbf{u}_2,\ldots,\; {}^0\mathbf{T}_k\,{}^k\mathbf{u}_k,\; \mathbf{0}\,] \qquad\qquad k = 1,\ldots,N \tag{5}$$

The vector ${}^i\mathbf{u}_i$ is the unit column vector in frame i parallel to the revolute axis through joint i, and **0** is a 3×(N-k) zero element matrix. The end-effector angular velocity is simply given by:

$$\boldsymbol{\omega}_E \;=\; \boldsymbol{\omega}_N \tag{6}$$

It can be shown that in the absence of external torques, and for zero initial $\dot{\mathbf{r}}_{cm}$, the constant angular momentum of the system is given by the sum [9,11]:

$$\mathbf{h} \;=\; \sum_{j=0}^{N}\sum_{i=0}^{N} \mathbf{D}_{ij}\,\boldsymbol{\omega}_j \tag{7}$$

where $\mathbf{D}_{ij}$ are mixed inertia matrices, functions of the barycentric vectors, and given by Equation (A5). Assuming zero initial angular momentum, Equation (7) can be solved for ${}^0\boldsymbol{\omega}_0$ to yield:

$$ {}^0\boldsymbol{\omega}_0 = - {}^0\mathbf{D}^{-1}\, {}^0\mathbf{D}_{\mathbf{q}}\, \dot{\mathbf{q}} \tag{8} $$

where ${}^0\mathbf{D}$ is the 3×3 inertia matrix of the system expressed in the spacecraft frame at the system *CM*, and ${}^0\mathbf{D}_{\mathbf{q}}$ is a 3×N matrix that corresponds to the inertia of the system's moving parts, see Equations (A7). Note that the inverse of ${}^0\mathbf{D}$ always exists because the system inertia matrix is positive definite.

Equation (8) can be used to eliminate the spacecraft angular velocity ${}^0\boldsymbol{\omega}_0$ from Equations (3) and (6), and hence to derive a free-floating system's Jacobian $\mathbf{J}^*$, defined by:

$$ [\, \dot{\mathbf{r}}_E\, , \boldsymbol{\omega}_E \,]^T = \mathbf{J}^*\, \dot{\mathbf{q}} \tag{9} $$

and given as:

$$ \mathbf{J}^*(\boldsymbol{\Theta},\mathbf{q}) = \mathrm{diag}(\mathbf{T}_0,\mathbf{T}_0)\; {}^0\mathbf{J}^*(\mathbf{q}) \tag{10} $$

$$ {}^0\mathbf{J}^*(\mathbf{q}) \equiv \begin{bmatrix} - {}^0\mathbf{J}_{11}\, {}^0\mathbf{D}^{-1}\, {}^0\mathbf{D}_{\mathbf{q}} + {}^0\mathbf{J}_{12} \\ - {}^0\mathbf{D}^{-1}\, {}^0\mathbf{D}_{\mathbf{q}} + {}^0\mathbf{J}_{22} \end{bmatrix} \tag{11} $$

where the matrices ${}^0\mathbf{J}_{11}$, ${}^0\mathbf{J}_{12}$, and ${}^0\mathbf{J}_{22}$, are defined in Appendix A.

Note that these Jacobians are *basic Jacobians*, that is Jacobians independent of the particular parameter set used to describe the end-effector orientation [14]. Kinematic equations related to the particular orientation representation also must be used. Equation (9) describes the effect of joint motions on end-effector velocities, and its form is the same to the form that of that for fixed-based systems. Comparing the structure of ${}^0\mathbf{J}^*$ to the structure of the Jacobian $\mathbf{J}$, that would be written for the same manipulator but with a fixed base, it is easy to see that these are the same. Indeed, both depend on the configuration $\mathbf{q}$, and have the same size, 6×N. The same observations hold for $\mathbf{J}^*$, with the exception that in addition, this is also a function of the spacecraft orientation. However, this orientation can be estimated or measured, and hence, $\mathbf{J}^*$ can be used in the place of $\mathbf{J}$ in well-established control or planning algorithms derived for fixed-based systems.

Note that $\mathbf{J}^*$ depends not only on the kinematic properties of the system, but also on configuration dependent mass properties, eg. inertias. This observation suggests that singular configurations for a free-floating system, i.e. ones in which ${}^0\mathbf{J}^*$ has rank less than six, will not be the same to the ones for fixed based systems. This is indeed the case, as we will see later.

B. Dynamic Modelling

To derive the equations of motion of a free-floating system, the system kinetic energy is expressed as a function of the generalized coordinates and their velocities, [10,11].

$$T = \frac{1}{2} \sum_{j=0}^{N} \sum_{i=0}^{N} \boldsymbol{\omega}_i^T \mathbf{D}_{ij} \boldsymbol{\omega}_j \tag{12}$$

It can be shown that under the same assumptions as above, T is given by [10,11]:

$$T = \frac{1}{2} \dot{\mathbf{q}}^T \mathbf{H}^*(\mathbf{q}) \dot{\mathbf{q}} \tag{13}$$

where $\mathbf{H}^*(\mathbf{q})$ is the *reduced* system inertia matrix, given by:

$$\mathbf{H}^*(\mathbf{q}) \equiv {}^0\mathbf{D}_{\mathbf{qq}} - {}^0\mathbf{D}_{\mathbf{q}}^T \, {}^0\mathbf{D}^{-1} \, {}^0\mathbf{D}_{\mathbf{q}} \tag{14}$$

The matrices ${}^0\mathbf{D}$, ${}^0\mathbf{D}_{\mathbf{q}}$, and ${}^0\mathbf{D}_{\mathbf{qq}}$ are defined by Equations (A7). It is easy to show that the system inertia matrix, $\mathbf{H}^*$, is an N×N positive definite symmetric inertia matrix, which depends on $\mathbf{q}$ and the system mass and inertia properties. All elements of $\mathbf{H}^*$ are functions of the manipulator joint angles q_i (i=1,...,N) only, since ${}^0\mathbf{D}$, ${}^0\mathbf{D}_{\mathbf{q}}$, and ${}^0\mathbf{D}_{\mathbf{qq}}$ are functions of only the q_i's and not of the spacecraft attitude; hence the system inertia matrix $\mathbf{H}^*$ has the same structural properties as the inertia matrices that correspond to fixed-base manipulators.

In the absence of gravity, the potential energy of a rigid system is zero, and the system's dynamic equations are given by:

$$\frac{d}{dt} \left\{ \frac{\partial T}{\partial \dot{\mathbf{q}}} \right\} - \frac{\partial T}{\partial \mathbf{q}} = \boldsymbol{\tau} \tag{15}$$

where $\boldsymbol{\tau}$ is the generalized force vector which, in this case, is equal to the torque vector $[\, \tau_1, \tau_2, ..., \tau_N \,]^T$. Applying Equation (15) to the kinetic energy given by Equation (13) results in a set of N equations of motion of the form:

$$\mathbf{H}^*(\mathbf{q}) \ddot{\mathbf{q}} + \mathbf{C}^*(\mathbf{q}, \dot{\mathbf{q}}) \dot{\mathbf{q}} = \boldsymbol{\tau} \tag{16}$$

where $\mathbf{H}^*(\mathbf{q})$, is the system inertia matrix defined by Equation (14) and $\mathbf{C}^*(\mathbf{q}, \dot{\mathbf{q}}) \dot{\mathbf{q}}$ contains nonlinear centrifugal and Coriolis terms. Note that the equations of motion are written as functions of the joint variables only, and not of the spacecraft variables. This results from the fact that the system kinetic energy does not depend on a spacecraft's attitude nor on its angular or linear velocity, when the system initial angular momentum is zero, and the system is free of external torques. The spacecraft's contribution to the system's kinetic energy, T, enters in through the inertia matrices ${}^0\mathbf{D}$ and ${}^0\mathbf{D}_{\mathbf{q}}$, which depend on its mass m_0 and inertia $\mathbf{I}_0$.

If it is assumed that a particular task requires motion control of the end-effector, then Equations (9) and (16) can be used to design a controller. Based on the structural similarity of these equations to the ones derived for a fixed based system,

Reference [10] suggested that if singularities of $\mathbf{J}^*$ can be avoided, nearly any control algorithm applied to fixed-based systems can be used in free-floating systems. The nature of free-floating system singularities and workspaces, in conjunction to the nonintegrability of the angular momentum, is addressed next.

III. Controllability, Dynamic Singularities and Workspaces

A. Controllability in the Joint Space

Assume that one task requires control of the system configuration $\mathbf{q}$, only. Then, a linearizing feedforward control law of the form $\boldsymbol{\tau} = \mathbf{H}^*(\mathbf{q})\ \mathbf{u} + \mathbf{C}^*(\mathbf{q}, \dot{\mathbf{q}})\ \dot{\mathbf{q}}$, where $\mathbf{u} \in \mathbf{R}^N$ is an auxiliary control input, reduces the equations of motion to a controllable decoupled second order system. This can be done because $\mathbf{H}^*$ is a positive definite matrix, and proves that the system is controllable in its joint space.

B. Nonintegrability of the Angular Momentum

The angular momentum, given by Equation (8), cannot be integrated to yield the spacecraft's orientation as a function of the system's configuration, $\mathbf{q}$, with the exception of a planar two body system [11]. Obviously, this equation can be integrated numerically, but in such a case the resulting final spacecraft orientation will be a function of the path taken in the joint space. In other words, different paths in the joint space, with the same initial and final points, will result in different spacecraft orientations. Due to Equation (9), the same applies to workspace paths; i.e. moving from one workspace location to another one via different paths results in different final spacecraft orientations. Closed paths in the joint space or the workspace can change the system's attitude.

It is this nonintegrability property that introduces nonholonomic characteristics to free-floating systems. However, this nonholonomic behavior results from the particular *dynamic* structure of the system, and is not due to *kinematic* nonintegrable constraints, like the ones experienced by a rolling disk. The use of this nonholonomic behavior to achieve various tasks is described in the following sections.

C. Controllability in the Cartesian Space

Assume next that the task is to move the end-effector to some position and orientation, and that N = 6. Since the system is controllable in its joint space, any $\mathbf{q}$, $\dot{\mathbf{q}}$ can be obtained. The question that arises next is wether this is enough to obtain any $\dot{\mathbf{r}}_E$, $\boldsymbol{\omega}_E$, and eventually any position and orientation. The answer to this question is affirmative if the Jacobian $\mathbf{J}^*$ is of full rank, i.e. six. Similar observations hold for the more general case of an N DOF manipulator. Since the transformation matrix $\mathbf{T}_0$ is not singular, (with the exception of possible representation singularities), then $\mathbf{J}^*$ looses its full rank when:

$$\det[{}^0\mathbf{J}^*(\mathbf{q})] = 0 \qquad (17)$$

The above condition shows that singularities in free-floating systems are fixed in joint space. However, since ${}^0\mathbf{J}^*$ is a function of configuration dependent inertia matrices, these singularities are different than the ones for fixed base systems, and their location in joint space depend in addition on the dynamic properties of the system; for these reasons, they were called *dynamic singularities* [9].

It is interesting to examine the location of the dynamic singularities in a system's workspace. To do this we need a one to one correspondence from the joint space to the cartesian workspace. However, such a correspondence does not exist, even in the case of a six DOF manipulator, because its end-effector position $\mathbf{r}_E$, and orientation $\mathbf{T}_E$, are not only functions of the system's configuration $\mathbf{q}$, but also of the path dependent spacecraft orientation, $\boldsymbol{\theta}$, see also Equations (1) and (2):

$$\mathbf{r}_E(\boldsymbol{\theta}, \mathbf{q}) = \mathbf{T}_0(\boldsymbol{\theta}) \sum_{i=0}^{6} {}^0\mathbf{T}_i \, {}^i\mathbf{v}_{i6,E} \tag{18}$$

$$\mathbf{T}_E(\boldsymbol{\theta}, \mathbf{q}) = \mathbf{T}_0(\boldsymbol{\theta}) \, {}^0\mathbf{T}_6(q_1, \ldots, q_6) \tag{19}$$

The ${}^i\mathbf{v}_{i6,E}$ are constant vectors. Out of all the pairs ($\boldsymbol{\theta}$, $\mathbf{q}$) with which a workspace point can be reached, some may correspond to a singular configuration, $\mathbf{q}_s$. Then a workspace point may or may not induce a dynamic singularity, depending on the joint space path taken to reach it.

To resolve this ambiguity, *Path Dependent Workspaces* (PDW) were defined to contain all workspace locations that may induce a dynamic singularity [9,11]. To find these points, note that the distance of a workspace location from the system *CM* does not depend on the spacecraft's orientation:

$$R = R(\mathbf{q}) = \left\| \sum_{i=0}^{N} {}^0\mathbf{T}_i \, {}^i\mathbf{v}_{i6,E} \right\| \tag{20}$$

This equation represents a spherical shell in the workspace. All the singular configurations $\mathbf{q}_s$ are mapped through Equation (20) to a set of shells, whose union gives the PDW. If we subtract the PDW from the reachable workspace, contained in a spherical volume defined by:

$$R_{min} = \min_{\mathbf{q}} \; R(\mathbf{q}) \tag{21a}$$

$$R_{max} = \max_{\mathbf{q}} \; R(\mathbf{q}) \tag{21b}$$

we get the *Path Independent Workspace*, (PIW). All points in the PIW are guaranteed not to induce dynamic singularities. Then, any point in the PIW can be reached from all other points in the PIW, by any path that belongs entirely to the PIW.

If the system is in a dynamically singular configuration, the end-effector is constrained to move on a manifold of dimension lower than six. This means that

some workspace points are not reachable with small $\delta\mathbf{q}$, whatever $\delta\mathbf{q}$ is. In other words, the system is locally uncontrollable. However, it may still be possible to reach any PDW point from any other workspace point, by choosing an appropriate path. This will be demonstrated in the following sections.

C. Controllability in the State Space

A system with a 6 DOF manipulator has 12 DOF, the additional six corresponding to the position and orientation of the spacecraft. Assuming an Euler angle representation of a spacecraft's orientation, a state space can be formed containing the position and orientation of the spacecraft, the joint angles or the end-effector position and orientation, and the corresponding velocities or rates. The dimension of such a state space is 2·12. However, since the linear momentum can be integrated to yield a spacecraft's position as a function of the manipulator links, one cannot set the position of the spacecraft independently of the position of the manipulator links. This shows that the controllable subspace has dimension at most 2·9. In addition, due to the angular momentum given by Equation (8), a spacecraft's angular velocity cannot be specified independently of the joint rates $\dot{\mathbf{q}}$. Hence, the controllable subspace is at most of dimension 2·9-3=15. Although the exact dimension of the controllable subspace has not been established yet, it has been shown by specific examples that it is possible to control a spacecraft's orientation, in addition to the manipulator joint variables, by employing special joint space paths.

IV. Example

Consider the planar free-floating space manipulator shown in Figure 2. The system parameters are given in Table I. For this system, vectors $\mathbf{r}_i$ and $\mathbf{l}_i$ that connect a link's *CM* to its two joints, see Figure 1, are parallel to the x axis of the i^{th} frame. Hence, only the x-component of the barycentric vectors in Equation (A1) is non-zero, and is given by:

$$
\begin{aligned}
{}^0v_{02,E} &\equiv \alpha = \frac{1}{M}\, r_0 m_0 = 0.426 \text{ m} \\
{}^1v_{12,E} &\equiv \beta = \frac{1}{M}\, \{r_1(m_0+m_1)+l_1 m_0\} = 0.894 \text{ m} \\
{}^1v_{22,E} &\equiv \gamma = \frac{1}{M}\, l_2(m_0+m_1) + r_2 = 0.968 \text{ m}
\end{aligned}
\tag{22}
$$

where M is the total system mass, $M = m_0 + m_1 + m_2$. For this system, only the position of the end-effector, $\mathbf{r}_E = [x, y]^T$, is controlled. This position is written using Equation (18) as:

$$
\begin{aligned}
x &= \alpha\cos(\theta) + \beta\cos(\theta+q_1) + \gamma\cos(\theta+q_1+q_2) \\
y &= \alpha\sin(\theta) + \beta\sin(\theta+q_1) + \gamma\sin(\theta+q_1+q_2)
\end{aligned}
\tag{23}
$$

where θ, q_1 and q_2, are defined in Figure 2. As shown in [9], the system Jacobian is:

$$\mathbf{J}^*(\theta,\mathbf{q}) = \mathbf{T}_0(\theta)\,{}^0\mathbf{J}^*(\mathbf{q}) = \begin{bmatrix}\cos(\theta) & -\sin(\theta)\\ \sin(\theta) & \cos(\theta)\end{bmatrix}{}^0\mathbf{J}^*(\mathbf{q}) \quad (24a)$$

$${}^0\mathbf{J}^*(\mathbf{q}) = \frac{1}{D}\begin{bmatrix} -(\beta s_1+\gamma s_{12})D_0 & \beta s_1 D_2-\gamma s_{12}(D_0+D_1) \\ -\alpha(D_1+D_2)+(\beta c_1+\gamma c_{12})D_0 & -(\alpha+\beta c_1)D_2+\gamma c_{12}(D_0+D_1)\end{bmatrix} \quad (24b)$$

where $s_1 = \sin(q_1)$, $c_{12} = \cos(q_1+q_2)$ etc. The inertia scalar sums D, D_0, D_1 and D_2 are defined in Appendix B, see Equation (B2). Since each D_i (i=0,1,2) and D are functions of **q**, the Jacobian elements are more complicated functions of the **q** than their fixed-base counterparts. Note that D represents the inertia of the whole system with respect to its *CM* and thus, is always a positive number.

Table I. The system parameters.

Body	l_i (m)	r_i (m)	m_i (Kg)	I_i (Kg m^2)
0	.5	.5	40	6.667
1	.5	.5	4	0.333
2	.5	.5	3	0.250

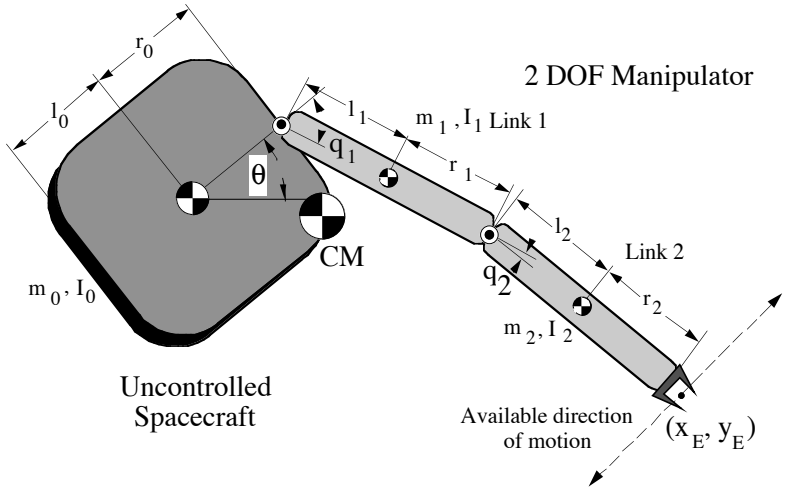

Figure 2. A planar 2 DOF free-floating manipulator, shown in a dynamically singular configuration.

The system inertia matrix, $\mathbf{H}^*$, is found according to Equations (14), (B1), and (B2). The result is:

$$\mathbf{H}^*(\mathbf{q}) = \begin{bmatrix} {}^0d_{11}+2{}^0d_{12}+{}^0d_{22}-\dfrac{(D_1+D_2)^2}{D} & {}^0d_{12}+{}^0d_{22}-\dfrac{D_2(D_1+D_2)}{D} \\ {}^0d_{12}+{}^0d_{22}-\dfrac{D_2(D_1+D_2)}{D} & {}^0d_{22}-\dfrac{D_2^2}{D} \end{bmatrix} \tag{25}$$

where the mixed inertia terms ${}^0d_{ij}$ are defined in Appendix B. Note that $\mathbf{H}^*$ is a 2×2 positive definite symmetric matrix whose elements are functions of the joint angles q_1 and q_2, and its size and structure is the same to the inertia matrix of a fixed base system. Hence, as discussed above, it is easy to show that the example system is controllable in its joint space.

The zero angular momentum for this system is written using Equation (8) as:

$$D\dot{\theta} + (D_1+D_2)\,\dot{q}_1 + D_2\,\dot{q}_2 = 0 \tag{26}$$

Multiplying both sides by dt, a Pfafian equation results. This Pfafian can only be integrated if the following condition holds [15]:

$$D\left\{\frac{\partial(D_1+D_2)}{\partial q_2} - \frac{\partial D_2}{\partial q_1}\right\} - (D_1+D_2)\,\frac{\partial D}{\partial q_2} + D_2\,\frac{\partial D}{\partial q_1} = 0 \tag{27}$$

However, after some algebra one can show that this condition does not hold, and therefore, the angular momentum cannot be integrated to yield θ as a function of q_1 and q_2. Nonholonomic behavior is expected for this system.

The system Jacobian becomes singular, when its determinant is zero. This condition results in the following equation:

$$\alpha\beta D_2\sin(q_1)+\beta\gamma D_0\sin(q_2)-\alpha\gamma D_1\sin(q_1+q_2) = 0 \tag{28}$$

The values of q_1 and q_2 which satisfy Equation (28) and result in dynamically singular configurations can be plotted in joint space as shown in Figure 3. This figure also shows that conventional kinematic singularities like $q_1=k\pi$, $q_2=k\pi$, $k=0,\pm1,\ldots$ still satisfy Equation (28). However, infinitely more dynamically singular configurations exist which cannot be predicted from the kinematic structure of the manipulator.

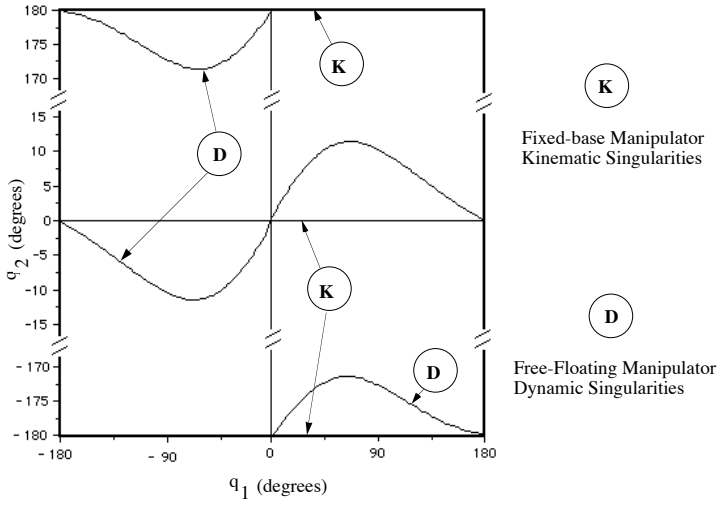

Figure 3. Dynamically singular configurations for the system shown in Figure 2.

Figure 3 shows the system in the singular configuration at q_1=-65°, q_2=-11.41°, and the spacecraft attitude at θ=40°. In this configuration, the local inertial motion of the end-effector will be the shown in the figure, no matter how the joint actuators are driven, and the system is locally uncontrollable. The best a control algorithm can do at such a point is to follow the available direction. *All* algorithms that use a Jacobian inverse, such as the resolved rate or resolved acceleration control algorithms, fail at such a point. Ones that use a pseudoinverse Jacobian or a Jacobian transpose will likely follow the available direction, but may result in large errors.

To find the limits of the reachable workspace, the distance R of the end-effector from the system *CM* given by Equation (20) is written as:

$$R = R(\mathbf{q}) = \sqrt{\alpha^2 + \beta^2 + \gamma^2 + 2\alpha\beta\cos(q_1) + 2\alpha\gamma\cos(q_1+q_2) + 2\beta\gamma\cos(q_2)} \tag{29}$$

For this example, the reachable workspace is the area confined between two circles with radii:

$$R_{min} = 0.352 \text{ m} = \alpha+\beta-\gamma \tag{30a}$$

$$R_{max} = 2.288 \text{ m} = \alpha+\beta+\gamma \tag{30b}$$

while the PIW is confined between the circles with radii:

$$R_1 = 0.554 \text{ m} \tag{31a}$$

$$R_2 = 1.436 \text{ m} \tag{31b}$$

Figure 4 depicts the reachable, PDW, and PIW spaces for this example. When the end-effector path has points belonging to the PDW, such as path B in Figure 4, the manipulator may assume a dynamically singular configuration, depending on the

path. On the other hand, paths totally within the PIW region, such as path A, can never lead to dynamically singular configurations.

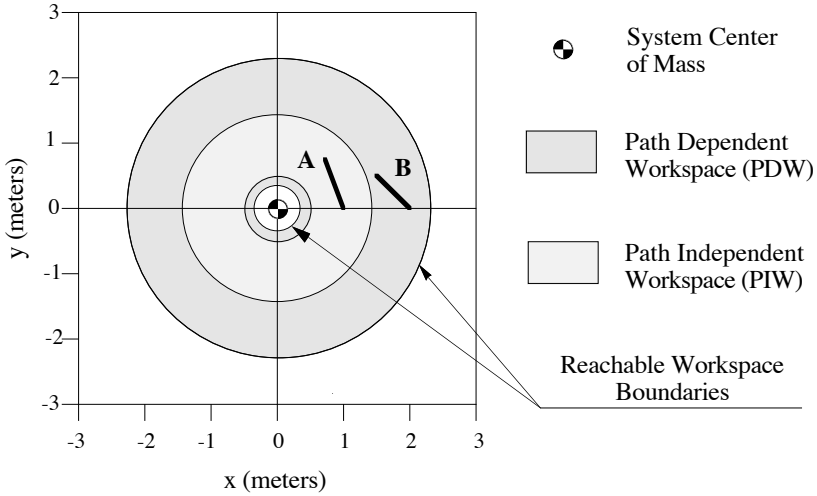

Figure 4. The reachable, Path Dependent, and Path Independent Workspaces, for the system shown in Figure 2.

In the next section we explore the use of the nonholonomic behavior of a free-floating system in planning to achieve various tasks.

V. Path Planning in Joint Space

a. Self Correcting Planning

A free-floating system may operate under the Spacecraft-Referenced End-Point Motion Control, in which either the manipulator end-point is commanded to move to a location fixed to its own spacecraft, or a simple joint motion is commanded, such as when the manipulator is to be driven at its stowed position [10]. In general, a manipulator's motion in joint space will change the spacecraft's orientation, as discussed above. However, there are many cases in which this phenomenon may be highly undesirable. For example, the spacecraft may be required to maintain a constant orientation for communication purposes. Therefore, it would be useful to control a system's orientation, without using limited thruster fuel.

Due to the nonholonomic behavior of a free-floating system, different joint space paths with the same initial and final points, will result in different spacecraft orientations. In addition, a closed path in the manipulator's joint space, will result in a net change in the spacecraft's orientation. Based on these observations, a Self Correcting Planning technique that can correct for any deviations from a desired orientation by executing closed joint space paths, has been proposed [2]. Here, the basic elements of this technique are reviewed.

If a spacecraft's orientation is described by the 3-2-1 Euler angles, $\Theta = [\theta_1,\theta_2,\theta_3]^T$, then these are written using Equation (8) as [16]:

$$\dot{\boldsymbol{\Theta}} = -\mathbf{S}^{-1}(\boldsymbol{\Theta})\,\boldsymbol{\omega}_0 = -\mathbf{S}^{-1}(\boldsymbol{\Theta})\,\mathbf{T}_0^{\,0}\mathbf{D}^{-1\ 0}\mathbf{D}_{\mathbf{q}}\dot{\mathbf{q}} = \mathbf{G}(\boldsymbol{\Theta}, \mathbf{q})\dot{\mathbf{q}} \tag{32}$$

where $\mathbf{S}^{-1}(\boldsymbol{\Theta})$ is a nonsingular matrix, except at some isolated points, and is given by:

$$\mathbf{S}^{-1}(\boldsymbol{\Theta}) = \begin{bmatrix} 1 & \sin\theta_1\sin\theta_2/\cos\theta_2 & \cos\theta_1\sin\theta_2/\cos\theta_2 \\ 0 & \cos\theta_1 & -\sin\theta_1 \\ 0 & \sin\theta_1/\cos\theta_2 & \cos\theta_1/\cos\theta_2 \end{bmatrix} \tag{33}$$

For small changes in the configuration $\mathbf{q}$, Equation (32) is written as:

$$\delta\boldsymbol{\Theta} = \mathbf{G}(\boldsymbol{\Theta}, \mathbf{q})\delta\mathbf{q} \tag{34}$$

where $\mathbf{G}$ is a 3×N matrix. Using a Taylor series expansion of Equation (34), and assuming a joint space closed path along the vectors $\delta\mathbf{V}$, $\delta\mathbf{W}$, $-\delta\mathbf{V}$, $-\delta\mathbf{W}$, the resulting change in the Euler angles $\delta\boldsymbol{\Theta}$ is given by [2]:

$$\delta\theta_i \approx \sum_{l=1}^{N}\sum_{m=1}^{N}\Big[\sum_{n=1}^{3}\Big(\frac{\partial G_{im}}{\partial\theta_n}G_{nl} - \frac{\partial G_{il}}{\partial\theta_n}G_{nm}\Big) + \frac{\partial G_{im}}{\partial q_l} - \frac{\partial G_{il}}{\partial q_m}\Big]\delta V_l\,\delta W_m \quad (i = 1,2,3) \tag{35}$$

Equation (35) can be used to find the joint space path, as described by vectors $\delta\mathbf{V}$, and $\delta\mathbf{W}$, to achieve a correction in the spacecraft's orientation by $\delta\boldsymbol{\Theta}$. Note that this is possible if at least one of the terms in brackets in Equation (35) is nonzero.

If the dimension of the manipulator's joint space is three, Equation (35) represents three equations in six unknowns, i.e. δV_i, δW_i, for i=1,2,3. The additional constraints:

$$\delta\mathbf{V}^T\,\delta\mathbf{W} = 0 \tag{36a}$$

$$\delta\mathbf{V}^T\,\delta\mathbf{V} = \delta\mathbf{W}^T\,\delta\mathbf{W} \tag{36b}$$

$$\delta V_3 = (\delta V_1 + \delta V_2)/2 \tag{36c}$$

allow complete determination of the required joint space path. This technique works well if $\delta\boldsymbol{\Theta}$ is small. If a large correction is required, this is broken in smaller ones, and more than one correction cycles are performed.

Example

Consider the system introduced in Section IV. It is desired to estimate the number of joint space closed square paths required to achieve a specified change in the spacecraft's orientation. For this system, $\mathbf{G}$ is a function of the configuration $\mathbf{q}$ only:

$$\mathbf{G}(\mathbf{q}) = [G_1, G_2] = \Big[-\frac{(D_1+D_2)}{D}, -\frac{D_2}{D}\Big] \tag{37}$$

According to Equations (36), vectors $\delta\mathbf{V}$ and $\delta\mathbf{W}$ are chosen to be:

$$\delta\mathbf{V} = [\delta q, 0]^T \qquad \delta\mathbf{W} = [0, \delta q]^T \tag{38}$$

where δq represents a small change in a joint angle. Equation (35) reduces to:

$$\delta\theta = \left(\frac{\partial G_2}{\partial q_1} - \frac{\partial G_1}{\partial q_2}\right)\delta q^2 = g(q_1,q_2)\,\delta q^2 \tag{39}$$

where $g(q_1,q_2)$ is a measure of the influence of a closed joint path on a spacecraft's orientation, and given by:

$$g(q_1,q_2) = -2\,\frac{{}^0d_{01}D_2\tan(q_1)+{}^0d_{12}D_0\tan(q_2)-{}^0d_{02}D_1\tan(q_1+q_2)}{D^2} \tag{40}$$

Assuming that at some particular configuration $g(q_1,q_2)$ is nonzero, Equation (40) yields the change in orientation of the spacecraft as a function of the area of the closed joint space path. If this path is a square with side δq, the number of paths required to achieve a change $\Delta\theta$ in the orientation, is obtained from Equation (39) as:

$$m \approx \frac{\Delta\theta\ 180\infty}{(\delta q)^2\,\pi\,\bar{g}} \tag{41}$$

where both $\Delta\theta$ and δq are in degrees, $\bar{g}$ is the value of $g(q_1,q_2)$ evaluated at $(q_1+\delta q/2, q_2+\delta q/2)$, and $\pi=3.14$.

To demonstrate the use of Equation (41), assume that the system is at $(\theta,q_1,q_2) = (14°,-48°,145°)$. Then $\bar{g} = g(-43°,150°) = -0.0495$. If the desired final θ is 10°, then $\Delta\theta = -4°$. Assuming a square joint path of side $\delta q = 10°$, and using Equation (41), we find that the required number of square paths is m = 46. Figure 5 shows the orientation as a function of m. After the execution of 46 closed joint paths, the spacecraft's orientation becomes 10.06°.

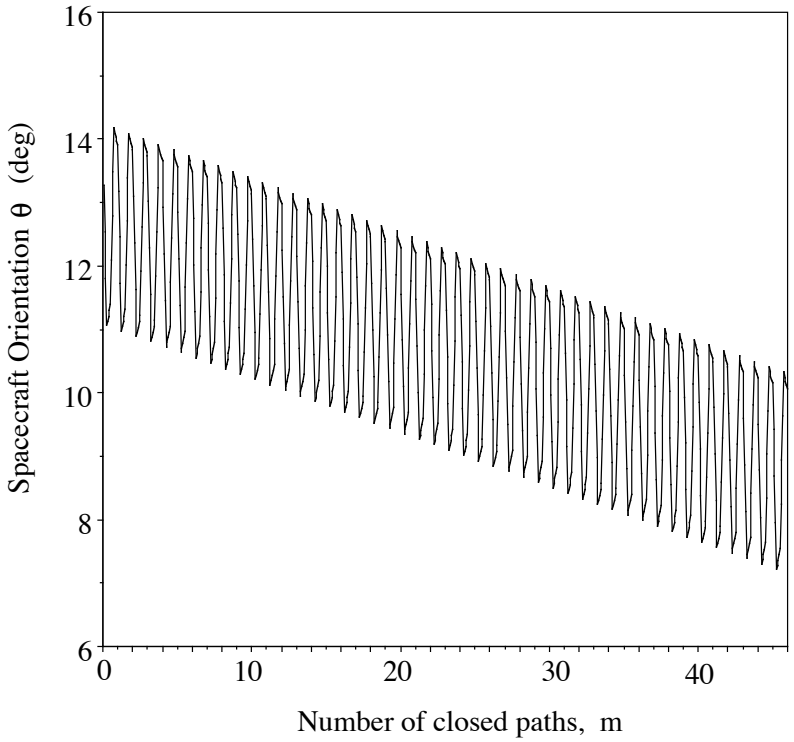

Figure 5. Changes in the spacecraft orientation θ, during the execution of closed joint space paths.

As discussed earlier, this self-correcting technique can be used if $\bar{g}$ is nonzero. However, $\bar{g}$ becomes zero for certain configurations **q**, shown in Figure 6. When the system manipulator is in one of these configurations, its spacecraft orientation cannot be affected by small joint space closed paths. These configurations can be mapped to cartesian space areas, using Equation (29) and the same procedure used for constructing the PDW. For this example, one can show that g is nonzero everywhere in the system's PIW. In other words, if the end-effector is in the PIW, the spacecraft orientation is always affected by closed joint space paths.

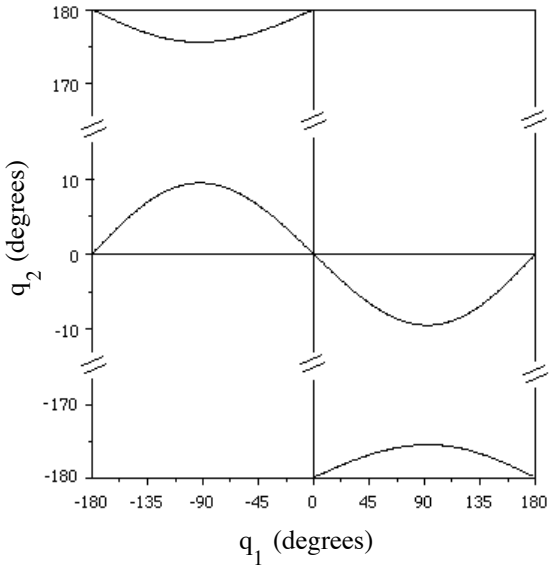

Figure 6. Configurations at which joint motions have no effect on the spacecraft's orientation θ.

b. Lyapunov-based Planning Techniques

In some cases, it is desirable to be able to control both a system's configuration **q**, and the orientation of its spacecraft, using joint motions only. A Lyapunov-based technique designed to achieve this goal was presented in References [7,8], and is reviewed here.

First, a vector $\mathbf{y} = [\Theta, \mathbf{q}]^T \in \mathbf{R}^{N+3}$, that contains the variables to be controlled is assembled. If the constant vector $\mathbf{y}_d$ denotes the desired **y**, the distance of the current **y** from the desired one is given by $\Delta\mathbf{y}$:

$$\Delta\mathbf{y} = \mathbf{y}_d - \mathbf{y} \tag{42}$$

Next, a Lyapunov function is constructed as follows:

$$V = \frac{1}{2} \Delta\mathbf{y}^T \mathbf{A} \Delta\mathbf{y} \tag{43}$$

where **A** is a positive definite matrix. V is positive, becoming zero only when $\Delta\mathbf{y}$ is zero. Since $\mathbf{y}_d$ is a constant, the time derivative of V is given by:

$$\dot{V} = -\Delta\mathbf{y}^T \mathbf{A} \dot{\mathbf{y}} \tag{44}$$

Using Equation (32), the following equation can be written for $\dot{\mathbf{y}}$:

$$\dot{\mathbf{y}} = \left[\mathbf{G}(\Theta, \mathbf{q}), \mathbf{I}\right]^T \dot{\mathbf{q}} = \mathbf{K}(\Theta, \mathbf{q})\dot{\mathbf{q}} \tag{45}$$

where **I** an N×N identity matrix, and **K** is an (N+3)×N matrix. Combining Equations (44) and (45), $\dot{V}$ becomes:

$$\dot{V} = -\Delta \mathbf{y}^T \mathbf{AK}\, \dot{\mathbf{q}} \tag{46}$$

and therefore, if one chooses $\dot{\mathbf{q}}$ according to:

$$\dot{\mathbf{q}} = (\mathbf{AK})^T \Delta \mathbf{y} \tag{47}$$

the time derivative of V is non-positive, since $\mathbf{AK}(\mathbf{AK})^T$ is positive semidefinite:

$$\dot{V} = -\Delta \mathbf{y}^T \mathbf{AK}\, (\mathbf{AK})^T \Delta \mathbf{y} \leq 0 \tag{48}$$

To guarantee that $\Delta\mathbf{y}$ will converge to zero, one must show that for nonzero $\Delta\mathbf{y}$, $\dot{V}$ is negative. However, as discussed in Reference [8], $(\mathbf{AK})^T$ has a null space, and $\Delta\mathbf{y}$ falls into it. In such a case, the motion stops, although $\Delta\mathbf{y}$ is nonzero.

To avoid this problem, a technique called the bi-directional approach has been proposed [8]. In this approach, two identical systems called 1 and 2, start at t=0 from the initial and final **y**. The error $\Delta\mathbf{y}$ is then defined as $\mathbf{y}_1 - \mathbf{y}_2$, where $\mathbf{y}_i$ corresponds to system i. If $\Delta\mathbf{y}$ is driven to zero, then system 1 follows in reverse the path followed by system 2, to reach the desired $\mathbf{y}_d$. Although this approach may reduce the chance of being caught by the null space of **K**, it does not eliminate it, and hence such a method should be employed with caution.

VI. Path-planning in the Cartesian Workspace

The previous techniques can be used to find joint paths that either correct a spacecraft's orientation during a manipulator's motion, or simultaneously control the spacecraft orientation, and the manipulator's configuration. However, in many important applications, the system will operate under an Inertially-Referenced End-Point Motion Control mode [10]. Here, the primary task is to move the end-effector of the manipulator, from one inertial location to another. As was shown in Section IV, this may be a problem if the path has segments in the PDW. These problems become even more serious when a load is captured by the end-effector, because in such a case, the PIW is reduced [11]. To avoid these problems, either the workspace should be restricted to the PIW, or a planning technique that avoids dynamic singularities should be employed. In this section, one such technique is developed.

Assume that the task is to move the end-effector from point A to point D, without encountering dynamic singularities that will prevent reaching the destination point. Then, the following strategy can be used:

(a) Start from the final desired spacecraft orientation and end-effector position/orientation, and move under joint space control to some point C of the PIW. Such a motion is not subject to the effects of dynamic singularities, because these

affect the cartesian motion, only. Record the path taken. The system reaches point C with $\mathbf{q}_{DC}$ and $\mathbf{\Theta}_{DC}$.

(b) Start from the initial desired spacecraft orientation and end-effector position/orientation, and move under joint space control to some point B of the PIW. The system reaches point C with $\mathbf{q}_{AB}$ and $\mathbf{\Theta}_{AB}$.

(c) Move from point B to point C, using any path. The system reaches point C with $\mathbf{q}_{AC}$ and $\mathbf{\Theta}_{AC}$. In general, these are different than $\mathbf{q}_{DC}$ and $\mathbf{\Theta}_{DC}$.

(d) Using small cyclical motions of the end-effector, change the spacecraft attitude from $\mathbf{\Theta}_{AC}$ to $\mathbf{\Theta}_{DC}$. The configuration changes from $\mathbf{q}_{AC}$ to $\mathbf{q}_{DC}$, since the end-effector does move around the same point in cartesian space.

(e) Use the recorded path during step (a), to move to point D.

The fact that small cyclical motions in the cartesian space can change a spacecraft's orientation is due to the following equation, obtained by combining Equations (10) and (32), and using an Euler angle representation for the end-effector orientation:

$$\delta\mathbf{\Theta} = \mathbf{G}(\mathbf{\Theta}, \mathbf{q})\left\{\text{diag}(\mathbf{I},\mathbf{S}^{-1}(\mathbf{\Theta}_E))\mathbf{J}^*\right\}^{-1}\delta\mathbf{x}_E = \mathbf{G}^*(\mathbf{\Theta}, \mathbf{x}_E)\,\delta\mathbf{x}_E \qquad (49)$$

where $\delta\mathbf{x}_E = \delta[\mathbf{r}_E,\mathbf{\Theta}_E]^T$ is a small change in the end-effector position/orientation. The 3×6 matrix $\mathbf{G}^*$ is written as a function of $\mathbf{\Theta}$, and $\mathbf{x}_E$, because if these are given, and if N=6, then $\mathbf{q}$ can be computed by inverting Equations (18) and (19). Note that Equation (49) has the same structure to Equation (35), though more complicated. Since $\mathbf{J}^*$ is invertible in the PIW, $\mathbf{G}^*$ exists and hence, closed paths in the cartesian space will result in changes in the orientation of a system's spacecraft. This technique is illustrated below by an example.

Example

Consider again the example system introduced in Section IV. The end-effector is initially at point A: (x,y) = (2,0), which belongs in the system's PDW, see Figure 7. The initial configuration of the system is $(q_1,q_2) = (-58°, 60.3°)$ which corresponds to an initial spacecraft orientation $\theta = 21°$. Assume that the end-effector is commanded to reach point D: (x,y) = (1.5,1.5). As the end-effector moves on a straight line from the initial to the desired location, a dynamic singularity occurs at point E where $(\theta,q_1,q_2) = (-32.4°, 74.24°, 10.6°)$, see Figure 7. The end-effector stops at this point if an inverse Jacobian planning or control algorithm is used, or deviates from the desired final point if a transposed Jacobian control algorithm is used [10,11].

Next, the algorithm introduced above is applied. The task is to reach point D, with $\theta \approx 3°$. This θ corresponds to $(q_1,q_2) = (39.4°, 22.2°)$. First, the end-effector is moved from the desired point D, to some PIW point C: (0.8, 0.5), see path DC in Figure 7. Here a straight line motion is used, and C is reached with θ_{DC}=49.1°, see Figure 8. Next, the end-effector is moved from the initial point A, to point B, which

for simplicity is taken equal to point C. The end-effector reaches point B: (0.8, 0.5) with $(\theta,q_1,q_2) = (14.5°, -49.4°, 145.9°)$. The next task is to change the orientation of the spacecraft, from θ_{AC}=14.5°, to θ_{DC}=49.1°. To this end, the end-effector is commanded to follow 11 circular paths, with radius .2m, as shown in Figure 7.

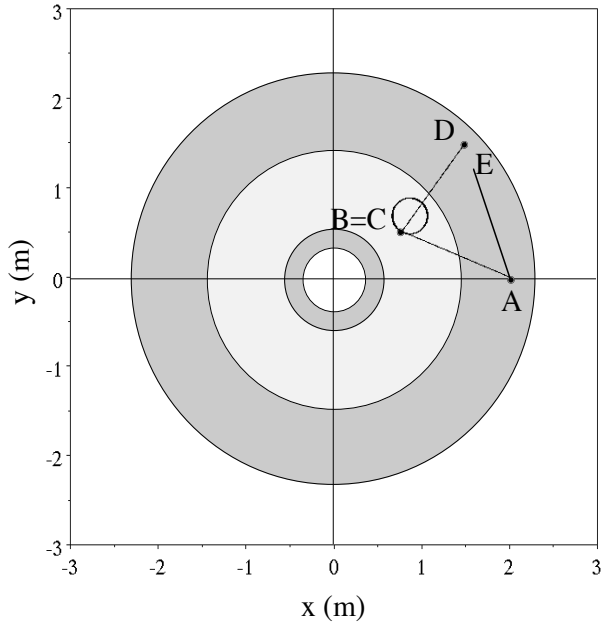

Figure 7. A Dynamic Singularity at point E does not allow the end-effector to move from point A to D. Path ABCD avoids singularities by employing small circles at point B.

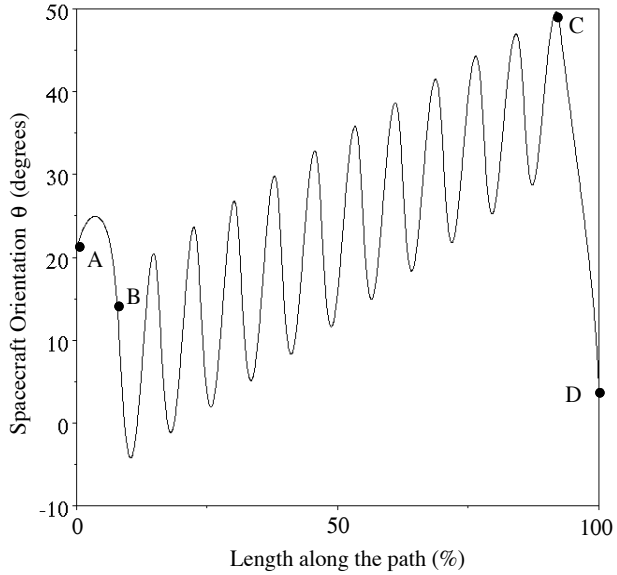

Figure 8. The orientation of the spacecraft θ as a function of the path ABCD, shown in Figure 7.

The required number of circles has been found by trial and error. After the execution of these circles, the orientation θ changes to 48.9°. Next, the end-effector is moved to D, following the prerecorded path DC in the opposite direction, and reaches D with $(\theta,q_1,q_2) = (3.3°, 38.9°, 22.7°)$. Note that not only point D, but also a final spacecraft orientation quite close to the desired one, have been reached. If a closer match in orientation is required, a smaller circle radius and more circles should be employed. Figure 8 depicts the change of θ during as a function of the length of the total path ABCD.

VII. Conclusions

The kinematics and dynamics of free-floating manipulators were examined from a fundamental point of view. It was shown that the dynamic coupling between the uncontrolled spacecraft and its manipulator can make the system dynamically singular at configurations which cannot be predicted by the system's kinematic properties. The nonintegrability of the angular momentum introduces nonholonomic behavior. A workspace point can induce a singularity or not, depending on the path taken to reach it. Trouble-free Path Independent Workspaces were defined. Two planning techniques that use nonholonomy to control a spacecraft's orientation by manipulator joint motions were reviewed. It was shown that in some system configurations, joint manipulator motions cannot affect a spacecraft's orientation. Finally, a planning method was presented that permits the effective use of a system's reachable workspace by planning paths which avoid dynamically singular configurations.

References

[1] Longman, R., Lindberg, R., and Zedd, M., "Satellite-Mounted Robot Manipulators-New Kinematics and Reaction Moment Compensation," *The Int. J. of Robotics Research,* Vol. 6, No. 3, pp. 87-103, Fall 1987.

[2] Vafa, Z., and Dubowsky, S., "On the Dynamics of Space Manipulators Using the Virtual Manipulator, with Applications to Path Planning," *J. of Astr. Sciences,* Vol. 38, No. 4, October-December 1990, pp. 441-472.

[3] Vafa, Z., and Dubowsky, S., "The Kinematics and Dynamics of Space Manipulators: The Virtual Manipulator Approach," *International Journal of Robotics Research*, Vol. 9, No. 4, August 1990, pp. 3-21.

[4] Alexander, H., and Cannon, R., "Experiments on the Control of a Satellite Manipulator," *Proc. 1987 American Control Conf.,* Seattle, WA, June 1987.

[5] Umetani, Y., and Yoshida, K., "Experimental Study on Two Dimensional Free-Flying Robot Satellite Model," *Proc. NASA Conf. on Space Telerobotics,* Pasadena, CA, January 1989.

[6] Masutani, Y., Miyazaki, F., and Arimoto, S., "Sensory Feedback Control for Space Manipulators," *Proc. of the IEEE Int. Conf. on Robotics and Automation*, Scottsdale, AZ, May 1989.

[7] Nakamura, Y., and Mukherjee, R., "Nonholonomic Path Planning of Space Robots," *Proc. of the IEEE Int. Conf. on Robotics and Automation*, Scottsdale, AZ, May 1989.

[8] Nakamura, Y., and Mukherjee, R., "Nonholonomic Path Planning of Space Robots via Bi-directional Approach," *Proc. of the IEEE Int. Conf. on Robotics and Automation*, Cincinnati, OH, May 1990.

[9] Papadopoulos, E., and Dubowsky, D., "On the Dynamic Singularities in the Control of Free-Floating Space Manipulators," *Proc. of the ASME Winter Annual Meeting*, San Fransisco, ASME DSC-Vol. 15, December 1989.

[10] Papadopoulos, E., and Dubowsky, S., "On the Nature of Control Algorithms for Free-floating Space Manipulators," *IEEE Trans. on Robotics and Automation*, Vol. 7, No. 6, December 1991, pp.750-758.

[11] Papadopoulos, E., "On the Dynamics and Control of Space Manipulators," Ph.D. Thesis, Department of Mechanical Engineering, MIT, October 1990.

[12] Hooker, W., and Margulies, G., "The Dynamical Attitude Equations for an n-Body Satellite," *J. of Astr. Sciences*, Vol XII, No 4, Winter 1965.

[13] Wittenburg, J., *Dynamics of Rigid Bodies,* B.G. Teubner, Stuttgart, 1977.

[14] Khatib, O., "A Unified Approach for Motion and Force Control of Robot Manipulators: The Operational Space Formulation," *IEEE Journal of Robotics and Automation*, Vol. RA-3, No. 1, February 1987, pp. 43-53.

[15] Korn, G., and Korn, T., *Mathematical Handbook for Scientists and Engineers*, Second Edition, McGraw-Hill, New York, NY, 1968.

[16] Hughes, P., *Spacecraft Attitude Dynamics*, John Wiley, New York, NY, 1986.

Appendix A

The general form of the barycentric vectors $\mathbf{v}_{ik}$ (i,k = 0…N) is [9,11]:

$$\mathbf{v}_{ik} \equiv \begin{cases} \mathbf{r}_i^* = -\mathbf{l}_i \sum_{j=0}^{i-1} \frac{m_j}{M} + \mathbf{r}_i \sum_{j=0}^{i} \frac{m_j}{M} & i<k \\ \mathbf{c}_i^* = -\mathbf{l}_i \sum_{j=0}^{i-1} \frac{m_j}{M} - \mathbf{r}_i \left(1-\sum_{j=0}^{i} \frac{m_j}{M}\right) & i=k \\ \mathbf{l}_i^* = \mathbf{l}_i \left(1-\sum_{j=0}^{i-1} \frac{m_j}{M}\right) - \mathbf{r}_i \left(1-\sum_{j=0}^{i} \frac{m_j}{M}\right) & i>k \end{cases} \qquad \text{(A1)}$$

where $\mathbf{l}_i$ and $\mathbf{r}_i$ are defined in Figure 1, m_i is the mass of body i, and M is the total system mass. Since $\mathbf{l}_i$ and $\mathbf{r}_i$ are body-fixed vectors, $\mathbf{v}_{ik}$ are also body-fixed. If ${}^i\mathbf{v}_{ik}$ are the barycentric vectors expressed in the i^{th} frame, then ${}^i\mathbf{v}_{ik}$ are constant vectors,

which can be computed only once. These are transformed in the inertial frame as follows:

$$\mathbf{v}_{ik} = \mathbf{T}_0 \, {}^0\mathbf{v}_{ik} = \mathbf{T}_0 \, {}^0\mathbf{T}_i \, {}^i\mathbf{v}_{ik} \tag{A2}$$

The vectors ${}^i\mathbf{v}_{iN}$, used in Equation (1) are obtained by setting k=N.

The matrices required for the construction of the Jacobian $\mathbf{J}^*$, see Equation (11), are functions of the vectors ${}^i\mathbf{v}_{iN,E} = {}^i\mathbf{v}_{iN} + \delta_{iN} \, {}^i\mathbf{r}_N$:

$${}^0\mathbf{J}_{11} \equiv -\sum_{i=0}^{N} [{}^0\mathbf{T}_i \, {}^i\mathbf{v}_{iN,E}]^{\times} \qquad {}^0\mathbf{J}_{12} \equiv -\sum_{i=1}^{N} [{}^0\mathbf{T}_i \, {}^i\mathbf{v}_{iN,E}]^{\times} \, {}^0\mathbf{F}_i \qquad {}^0\mathbf{J}_{22} \equiv {}^0\mathbf{F}_N \tag{A3}$$

where ${}^0\mathbf{F}_i$ (i = 1,…,N) are defined by Equation (5). The $^{\times}$ symbol operates on a column vector **e**, to form a skew-symmetric matrix which corresponds to a cross product:

$$\mathbf{e}^{\times} = \begin{bmatrix} 0 & -e_z & e_y \\ e_z & 0 & -e_x \\ -e_y & e_x & 0 \end{bmatrix} \tag{A4}$$

The mixed inertia matrices $\mathbf{D}_{ij}$ are also functions of the barycentric vectors [10,11]:

$$\mathbf{D}_{ij} \equiv \begin{Bmatrix} -M\{\mathbf{1}(\mathbf{l}^{*T}_j \mathbf{r}^{*}_i) - \mathbf{l}^{*}_j \mathbf{r}^{*T}_i\} & i<j \\ \mathbf{I}_i + \sum_{k=0}^{N} m_k \{\mathbf{v}_{ik}^{\,2} - \mathbf{v}_{ik}\mathbf{v}_{ik}^{\,T}\} & i=j \\ -M\{\mathbf{1}(\mathbf{r}^{*T}_j \mathbf{l}^{*}_i) - \mathbf{r}^{*}_j \mathbf{l}^{*T}_i\} & i>j \end{Bmatrix} \tag{A5}$$

where $\mathbf{v}_{ik}$, $\mathbf{r}^*_i$, and $\mathbf{l}^*_i$ are defined by Equation (A1). These mixed inertia matrices are transformed to a spacecraft's frame according to the following formula:

$$\mathbf{D}_{ij} = \mathbf{T}_0 \, {}^0\mathbf{D}_{ij} \, \mathbf{T}_0^{\,T} \qquad i, j = 1,...,N \tag{A6}$$

For simplicity, the following definitions are used:

$${}^0\mathbf{D}_j \equiv \sum_{i=0}^{N} {}^0\mathbf{D}_{ij} \qquad j = 0,...,N \qquad {}^0\mathbf{D} \equiv \sum_{j=0}^{N} {}^0\mathbf{D}_j \tag{A7a}$$

$${}^0\mathbf{D}_{\mathbf{q}} \equiv \sum_{j=1}^{N} {}^0\mathbf{D}_j \, {}^0\mathbf{F}_j \, {}^0\mathbf{D}_{\mathbf{qq}} \equiv \sum_{j=1}^{N} \sum_{i=1}^{N} {}^0\mathbf{F}_i^{\,T} \, {}^0\mathbf{D}_{ij} \, {}^0\mathbf{F}_j \tag{A7b}$$

Appendix B

For planar systems, the inertia matrices ${}^0\mathbf{D}_{ij}$ in Equations (A7) reduce to scalars ${}^0d_{ij}$ which are written as:

$$
\begin{aligned}
{}^0d_{00} &= I_0 + \frac{m_0(m_1+m_2)}{M}\, r_0^{\,2} \\
{}^0d_{10} &= \frac{m_0 r_0}{M}\,\{l_1(m_1+m_2) + r_1 m_2\}\cos(q_1) = {}^0d_{01} \\
{}^0d_{20} &= \frac{m_0 m_2}{M}\, r_0 l_2 \cos(q_1+q_2) = {}^0d_{02} \\
{}^0d_{11} &= I_1 + \frac{m_0 m_1}{M}\, l_1^{\,2} + \frac{m_1 m_2}{M}\, r_1^{\,2} + \frac{m_0 m_2}{M}(l_1+r_1)^{\,2} \\
{}^0d_{21} &= \left\{ \frac{m_1 m_2}{M}\, r_1 l_2 + \frac{m_0 m_2}{M}\, l_2(l_1+r_1)\right\}\cos(q_2) = {}^0d_{12} \\
{}^0d_{22} &= I_2 + \frac{m_2(m_0+m_1)}{M}\, l_2^{\,2}
\end{aligned}
\qquad \text{(B1)}
$$

The mixed inertia sum defined by Equations (A7) become:

$$
{}^0\mathbf{D}_j \equiv D_j = \sum_{i=0}^{2} {}^0d_{ij} \;\; (j=0,1,2) \qquad\qquad {}^0\mathbf{D} \equiv D = D_0 + D_1 + D_2
$$

$$
{}^0\mathbf{D}_\mathbf{q} = [D_1+D_2 \;\; D_2] \qquad\qquad {}^0\mathbf{D}_\mathbf{qq} = \begin{bmatrix} {}^0d_{11}+2{}^0d_{12}+{}^0d_{22} & {}^0d_{12}+{}^0d_{22} \\ {}^0d_{12}+{}^0d_{22} & {}^0d_{22} \end{bmatrix} \qquad \text{(B2)}
$$